Multiscale and Multiphysics Mechanics, *Vol. 1, No. 1 (2016) 35-51*
DOI: http://dx.doi.org/10.12989/mmm.2016.1.1.035

Estimation of a mixed-mode cohesive law for an interface crack between dissimilar materials

Sung-Il Song, Kwang-Soo Kim and Hyun-Gyu Kim*

Department of Mechanical and Automotive Engineering, Seoul National University of Science and Technology, 232 Gongneung-ro, Nowon-gu, Seoul, 139-743, Republic of Korea

(Received April 3, 2015, Revised October 8, 2015, Accepted October 22, 2015)

Abstract. In this paper, a mixed-mode cohesive law for an interface crack between epoxy and TR (transparent thermoplastic) resin is inversely estimated by the field projection method using numerical solutions and experimentally measured displacements. Displacements in a region far away from the crack tip are measured by digital image correlation technique. An inverse analysis, the field projection method formulated from the interaction J- and M-integrals with numerical auxiliary fields, is carried out to estimate a mixed-mode cohesive law for an interface crack between dissimilar materials. In the present approach, nonlinear deformations and damage near the crack tip are converted into the relationships of tractions and separations on crack surfaces behind the crack tip. The phase angle of mixed-mode singularities of the interface crack is also obtained from measured displacements in this study.

Keywords: cohesive laws; interface crack; mixed-mode singularity; inverse problem; field projection method

1. Introduction

The failure of an interface crack between bi-materials is an important issue in not only large-scale structures but also micro-scale structures such as adhesive joints, composite materials and microelectronics packages. In order to evaluate the failure characteristics of the interface crack, it is necessary to understand knowledge of the mechanical behaviors of a crack propagating along the bi-material interface. Elastic solutions around an interface crack-tip can be derived and the definition of the stress intensity factors has been discussed by previous researches (Williams 1959, Rice 1988, Erdogan 1965, England 1965, Rice and Sih 1965, Matos *et al*. 1989). In these solutions, the oscillatory stresses and the overlap of crack surfaces appear in the vicinity of a crack tip. In addition, it is necessary to define the phase angle of the mixed-mode singularity at the crack tip of bi-material interface, because it is considered that the mixed-mode fracture toughness depends on the phase angle (Hutchinson and Suo 1992). However, mixed-mode cohesive laws characterizing the failure behavior of a crack propagating along the interface between dissimilar materials have not been sufficiently investigated even though the evaluation of mixed-mode

*Corresponding author, Professor, E-mail: khg@seoultech.ac.kr

 ISSN: 2383-7306 (Print), 2465-9711 (Online)

cohesive laws is essential to simulate crack growth at bi-material interface.

The fracture energy, i.e., the energy for the crack growth, can be implemented in a cohesive model which connects crack surfaces with cohesive tractions using a traction-separation relation to describe the separation process between two surfaces. For mode I crack problems, the cohesive energy and the cohesive strength represent the local fracture toughness and local strength, respectively (Xu and Needleman 1994, Camacho and Ortiz 1996). The cohesive zone model has been widely applied to simulate delamination, crack propagation and failure process by pre-defining functional forms of cohesive laws (Ortiz and Pandolfi 1999, Mergheim *et al*. 2005). These previous studies showed successful results for simulating mode I fracture behavior efficiently in computational fracture mechanics. However, interface cracks between dissimilar materials require intrinsically mixed-mode cohesive laws which contain fracture energy, strengths in normal and shear separations. The normal and shear tractions on the crack surfaces between dissimilar materials should be related to the normal and shear separations as functions of loading conditions and material properties. Mixed-mode singularities at the crack tip are eliminated by applying cohesive tractions in the cohesive zone behind the crack tip of bi-material interface. The fracture energy of an interface crack is then implemented into the dissipation energy associated with normal and shear tractions and their separations. The interface fracture toughness under a loading condition has been measured by many researches (Xu and Tippur 1995, Ikeda *et al*. 1998, Liechti and Chai 1992, Yuuki *et al*. 1994). These researches reported that the fracture toughness increases with the phase angle and is closely dependent on the mode mixity. As a result, the phase angle of mixed-mode singularity at the crack tip of bi-material interface has been used as a parameter to determine mixed-mode cohesive laws.

Experimental estimate of cohesive laws near the crack tip is still highly non-trivial because the process zone size is very small and stresses cannot be measured directly, which requires measurements of the tractions and separations with high resolution and accuracy (Tan *et al*. 2005, Zhu *et al*. 2009). Indirect measurements of cohesive laws require an inverse process for finding unknown tractions and separations along crack surfaces from measured displacements or strains. A functional form of the traction-separation relationship is often assumed a priori, with the associated shape parameters as well as the cohesive energy, the cohesive strength and the separation length fitted to the measurement data (Zhu *et al*. 2009, Guo *et al*. 1999, Shen and Paulino 2011). While such approaches have been demonstrated convincingly, the accuracy of the experimentally fitted parameters is highly sensitive to the assumed traction-separation profile and an object function to match experimental results with simulations. Although the shape optimization approach minimizing an object function with a number of control points on the traction-separation curve (Shen and Paulino 2011, Gain *et al*. 2011) can be an affordable way to extract the cohesive law without a pre-defined form, sophisticated regularization techniques and experimental measurements in a region near the crack tip may be required to prevent from obtaining unphysical solutions due to the ill-posedness of inverse problems (Kim and Lee 2009). One promising method for reconstructing traction-separation relations from measured displacements without any pre-assumption on the shape of cohesive laws and comparing measured behaviors with model predictions for various parameters is the field projection method (FPM) (Hong and Kim 2003). The FPM constructs an inverse system by combining the interaction *J*-integral with analytical auxiliary fields along the contours in the cohesive zone and far-field region. The FPM was demonstrated to provide a systematic way of uncovering the shape of cohesive laws governed by the micro-mechanisms of the fracture process (Hong *et al*. 2009, Chew *et al*. 2009, Chalivendra *et al*. 2009). Numerical implementation of the FPM has been extended by

using numerical auxiliary fields (Kim *et al*. 2012). In this augmented FPM, discrete uniform tractions are systematically applied on each element face of the cohesive crack surfaces in turn to construct independent auxiliary fields. The use of both interaction *J*- and *M*-integrals in this method reduces the number of required auxiliary fields, compared to the previous method (Hong and Kim 2003). The cohesive laws for a crack in polymethly methacrylate (PMMA) double cantilever beam specimens have been successfully from experimentally measured displacements by using the augumented FPM (Oh and Kim 2013).

In this paper, we use the augumented FPM to extract a mixed-mode cohesive law for an interface crack between dissimilar materials. The displacements in a bi-material specimen made of epoxy and transparent thermoplastic (TR) resin mixtures are measured by using digital image correlation (DIC) technique. DIC can efficiently measure displacements in a region far away from the crack-tip during the crack growth. The measured data are transferred from measurement locations to finite element (FE) nodes by using moving least square (MLS) approximation. Inverse analyses formulated from the interaction *J*- and *M*-integrals with numerical auxiliary fields are carried out to extract a mixed-mode cohesive law for a crack growing along the bi-material interface from measured displacements in a far-field. Moreover, the phase angle of mixed-mode singularities of the interface crack from measured displacements is obtained in this study. The present hybrid procedure combining experimental measurements and the augmented FPM using numerical auxiliary fields can be an efficient way to estimate mixed-mode cohesive laws for a crack growth at the bi-material interface.

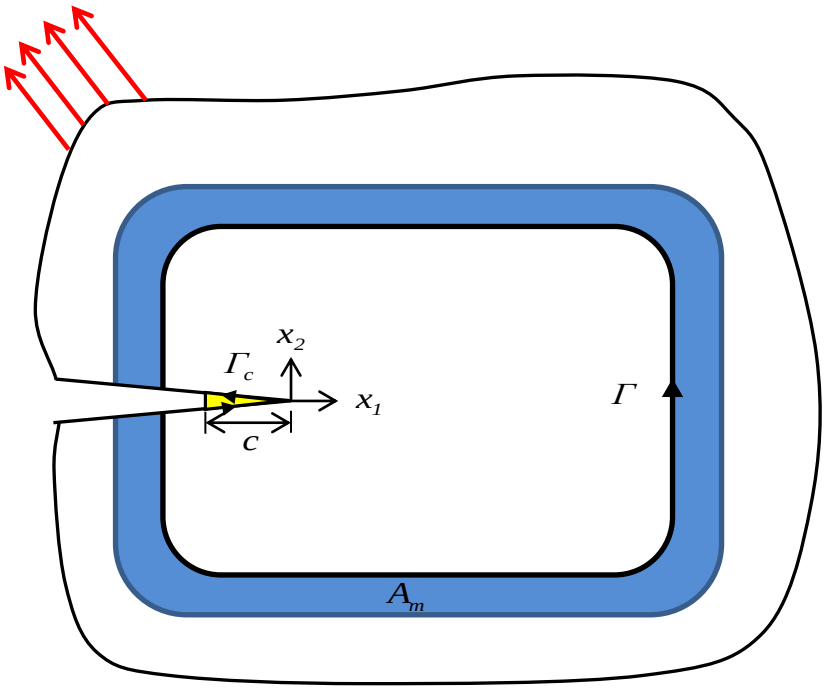

Fig. 1 Schematics of a cohesive zone of size c behind the cohesive crack tip. The interaction *J*- and *M*-integrals are taken over a remote path Γ, and are calculated using the domain integral method over the shaded region A_m

2. Field projection method using numerical auxiliary fields

In this study, a mixed-mode cohesive law for an interface crack is evaluated by using the FPM which inversely extracts tractions and separations on the crack surfaces from measured displacements in a far-field region. This algorithm has proven its usefulness for inversely extracting cohesive traction and separation values from measured displacements in a far-field region (Oh and Kim 2013). Fig. 1 illustrates an edge crack with a cohesive zone behind the crack tip. Since there is no singularity at the cohesive crack tip, *J*- and *M*-integrals at the cohesive crack surfaces Γ_c in Fig. 1 are equal to the values evaluated along arbitrary integral path Γ around the crack tip.

In order to extract unknown tractions and separations in the cohesive zone, Kim *et al.* (2012) used the interaction *J*- and *M*-integrals between the measured real field $S = S[\sigma_{ij}, u_{i,j}]$ and the auxiliary fields $\hat{S} = \hat{S}[\hat{\sigma}_{ij}, \hat{u}_{i,j}]$. The interaction *J*- and *M*-integrals along a path in a far-field region can be written by

$$J_{\Gamma}^{\text{int}}\left[S, \hat{S}\right] = \int_{\Gamma}\left(\sigma_{ij}\hat{u}_{i,j}n_1 - \sigma_{ij}\hat{u}_{j,1}n_i - \hat{\sigma}_{ij}u_{j,1}n_i\right)ds \tag{1}$$

$$M_{\Gamma}^{\text{int}}\left[S, \hat{S}\right] = \int_{\Gamma}\left(\sigma_{ij}\hat{u}_{i,j}n_k - \sigma_{ij}\hat{u}_{j,k}n_i - \hat{\sigma}_{ij}u_{j,k}n_i\right)x_k\, ds \tag{2}$$

Since the interaction integrals are path-independent and no singularity exists at the cohesive crack tip, the interaction integrals at the cohesive crack surfaces Γ_c can be rewritten as

$$J_{\Gamma_c}^{\text{int}}\left[S, \hat{S}\right] = -\int_{-c}^{0}\left(t_j\frac{\partial\Delta\hat{u}_j}{\partial x_1} + \hat{t}_j\frac{\partial\Delta u_j}{\partial x_1}\right)dx_1 \tag{3}$$

$$M_{\Gamma_c}^{\text{int}}\left[S, \hat{S}\right] = -\int_{-c}^{0}\left(t_j\frac{\partial\Delta\hat{u}_j}{\partial x_1} + \hat{t}_j\frac{\partial\Delta u_j}{\partial x_1}\right)x_1\, dx_1 \tag{4}$$

where t_j are the cohesive traction components on the lower crack surface, $\Delta u_j = u_j^+ - u_j^-$ are the separation components along the cohesive crack surfaces, and c is the length of the cohesive zone with the origin (x_1=x_2=0) located at the crack tip (see Fig. 1). By using the domain integral method (Shih *et al*. 1986) and the path independency of the interaction integrals such that $J_{\Gamma}^{\text{int}}[S, \hat{S}] = J_{\Gamma_c}^{\text{int}}[S, \hat{S}]$ and $M_{\Gamma}^{\text{int}}[S, \hat{S}] = M_{\Gamma_c}^{\text{int}}[S, \hat{S}]$, the relationship between the tractions and separations at the cohesive crack surfaces can be evaluated by

$$\int_{-c}^{0}\left(t_j\frac{\partial\Delta\hat{u}_j}{\partial x_1} + \hat{t}_j\frac{\partial\Delta u_j}{\partial x_1}\right)dx_1 = -\int_{A_m}\left(\sigma_{ij}\hat{u}_{j,1} + \hat{\sigma}_{ij}u_{j,1} - \sigma_{kl}\hat{u}_{k,l}\delta_{1i}\right)\frac{\partial q}{\partial x_i}\,dA \tag{5}$$

$$\int_{-c}^{0}\left(t_j\frac{\partial\Delta\hat{u}_j}{\partial x_1} + \hat{t}_j\frac{\partial\Delta u_j}{\partial x_1}\right)x_1\, dx_1 = -\int_{A_m}\left(\sigma_{ij}\hat{u}_{i,j}x_k + \hat{\sigma}_{ij}u_{j,k}x_k - \sigma_{kl}\hat{u}_{k,l}x_i\right)\frac{\partial q}{\partial x_i}\,dA \tag{6}$$

where q is an arbitrary continuous function with unit value on inner contour and zero value on outer contour, A_m is the integration domain as shown in Fig. 1, and summation over repeated

indices is implemented.

The *J*- and *M*-integrals can be defined for a cracked body with nonlinear deformation near the crack tip. As a result, the interaction integrals in Eqs. (1) and (2) give us characteristic values associated with nonlinear deformation and failure mechanisms at the crack tip. Hence, the cohesive laws extracted from measured displacements in a region far from the crack tip include both nonlinear material behavior near the crack tip and crack-bridging failure mechanisms, because the FPM in this study is based on a linear projection of far-fields data onto a local cohesive zone by using the conservation integrals in linear elastic materials.

In order to obtain the tractions and separations in cohesive law with a finite set of functions, a set of independent auxiliary fields should be provided for the interaction *J*- and *M*- integrals. In this study, we model the entire crack geometry with FE method, and systematically apply discrete uniform tractions on the element faces along the cohesive crack surfaces to generate the numerical auxiliary fields. Fig. 2 illustrates uniform normal and shear tractions that are applied separately on the faces of pair elements on the cohesive crack surfaces to establish independent auxiliary fields. Let $\hat{S}^{(K,i)}$ denote the numerical auxiliary fields generated by imposing uniform tractions such that

$$\hat{t}_j^{(K,i)}(x_1) = \begin{cases} \bar{t}^K \delta_{ij}, & x_1 \in C^K \\ 0, & \text{otherwise} \end{cases} \tag{7}$$

where C^K denote the faces of K^{th} elements in the cohesive zone, δ_{ij} is the Kronecker delta, and $\bar{t}^K$ are constant uniform tractions (see Fig. 2). Since the numerical auxiliary fields generated by different (*K*, *i*) combinations are mutually exclusive, we obtain independent auxiliary fields by applying discrete uniform tractions sequentially on cohesive crack surfaces in the finite element (FE) model. The objective of the inverse scheme is to determine the cohesive tractions and separations which are expressed as

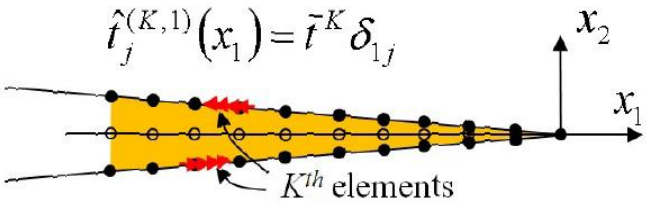

(a)

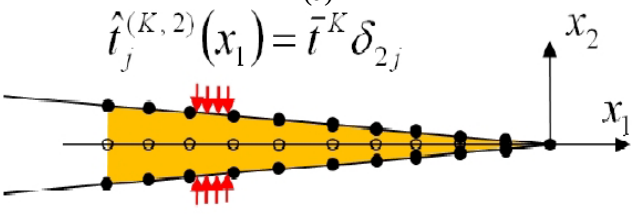

(b)

Fig. 2 Uniform shear and normal tractions imposed on the crack surfaces of the K^{th} element faces in the cohesive zone; the pseudo nodes are denoted by open circles

$$t_j(x_1) = t_j^E, \quad x_1 \in C^E \tag{8}$$

$$\Delta u_i(x_i) = \sum_{I=1}^{M+1} N^I(x_1)\Delta u_i^I, \quad \Delta u_i^{M+1} = 0 \tag{9}$$

where t_j^E are the unknown tractions, $E=(1,\cdots\cdots,M)$ are the element face numbers, $N^I(x_1)$ are the shape functions of virtual nodes *I*, and *M* is the total number of element pairs in the cohesive zone. The virtual nodes are defined at the center points between the actual nodes on the cohesive crack surfaces as denoted in Fig. 2. Constant tractions and linear separations on element faces in the cohesive zone are assumed, since linear quadrilateral elements are used in the FE computations. According to interaction formula such as $J_\Gamma^{\text{int}}[S,\hat{S}] = J_{\Gamma_c}^{\text{int}}[S,\hat{S}]$ and $M_\Gamma^{\text{int}}[S,\hat{S}] = M_{\Gamma_c}^{\text{int}}[S,\hat{S}]$ that can be expressed as

$$\sum_{E=1}^{M}\left[\int_{C^E}\frac{\partial\Delta\hat{u}_j^{(K,i)}}{\partial x_1}dx_1\right]t_j^E + \sum_{I=K}^{K+1}\left[\hat{t}_j^K\int_{C^K}\frac{\partial\Delta N^I}{\partial x_1}dx_1\right]\Delta u_j^I = -J_\Gamma^{\text{int}}(S,\hat{S}^{(K,i)}) \tag{10}$$

$$\sum_{E=1}^{M}\left[\int_{C^E}\frac{\partial\Delta\hat{u}_j^{(K,i)}}{\partial x_1}x_1\,dx_1\right]t_j^E + \sum_{I=K}^{K+1}\left[\hat{t}_j^K\int_{C^K}\frac{\partial\Delta N^I}{\partial x_1}x_1\,dx_1\right]\Delta u_j^I = -M_\Gamma^{\text{int}}(S,\hat{S}^{(K,i)}) \tag{11}$$

Finally, by solving the above equations, we can obtain the cohesive law in terms of tractions t_j^E and separations Δu_j^I on cohesive crack surfaces. It should be noted that the solutions of Eqs. (10) and (11) are not affected by the magnitude of uniform tractions in the auxiliary fields. Finally, by solving the inverse equations, we can obtain the cohesive law in terms of tractions t_j^E and separations Δu_j^I on cohesive crack surfaces.

3. Mixed-mode fracture at the crack tip

An asymptotic analysis of stresses and strains near the crack tip between dissimilar linear elastic solids shows that mixed-mode stress singularities exist at the bi-material interface crack tip. When a cohesive zone is involved on crack surfaces near the crack tip, the stress singularities at the cohesive crack tip can be disappeared because of finite normal and shear stresses at the initiation of separation. Nonetheless, the mixed-mode stress singularities at the bi-material interface crack tip can be related to the mixed-mode cohesive law of the interface crack, because the cohesive zone is confined in a very small region close to the crack tip (Jin and Sun 2005). For this reason, the phase angle associated with the mixed-mode stress singularities at the bi-material interface crack tip is obtained to characterize the cohesive zone in this study.

3.1 Stress intensity factors for an interface crack

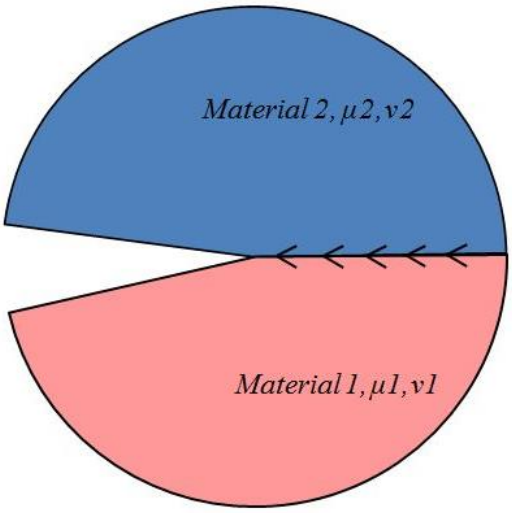

Fig. 3 An interface crack between dissimilar elastic materials

The stress field near the crack tip on the interface of two dissimilar elastic materials is defined as complex stress intensity factor K_1+iK_2 where i is the imaginary number. The stresses ahead of the interface crack on $x_2 = 0$ (Rice 1988) can be expressed as

$$\left(\sigma_{22} + i\sigma_{12}\right)_{\theta=0} = \frac{K_1 + iK_2}{\sqrt{2\pi r}} r^{i\varepsilon} \tag{12}$$

with

$$\varepsilon = \frac{1}{2\pi} ln\left(\frac{1-\beta}{1+\beta}\right) \tag{13}$$

$$\beta = \frac{1}{2} \frac{\mu_1(\kappa_2 - 1) - \mu_2(\kappa_1 - 1)}{\mu_1(\kappa_2 + 1) + \mu_2(\kappa_1 + 1)} \tag{14}$$

where μ_i are the shear moduli and ν_i are the Poisson's ratios of two linear elastic materials indicated in Fig. 3. $\kappa = (3-\nu)/(1+\nu)$ for plane stress and $\kappa = 3-4\nu$ for plane strain. The Dundurs parameter β is defined to calculate ε which is a bi-material constant causing oscillation stress singularity. As it is clear from Eq. (12), K_1 and K_2 do not longer reflect the cracking modes I and II because of the oscillatory term $r^{i\varepsilon}$. When the two materials are identical, $\varepsilon = 0$, the factors K_1 and K_2 become identical to conventional stress intensity factors K_I and K_{II}, respectively.

In order to separate the stress intensity factors in mode I and II, a similar stress intensity factors K_I and K_{II} which characterize the near tip stress field at an interface (Rice 1988) was introduced as,

$$K_I + iK_{II} = K\, l^{i\varepsilon} = |K|\, exp(i\psi), \;\; |K| = \sqrt{K_1^2 + K_2^2} \tag{15}$$

where l is the characteristic length ahead of the crack tip. The characteristic length can be chosen arbitrary. The state of stress near the crack tip is then characterized by the stress intensity factors

and the phase angle. The stress field in Eq. (12) can be rewritten as

$$\left(\sigma_{22}+i\sigma_{12}\right)_{\theta=0}=\frac{K_I+iK_{II}}{\sqrt{2\pi r}}\left(\frac{r}{l}\right)^{i\varepsilon} \tag{16}$$

3.2 Phase angle for a cohesive crack tip

The phase angle expressed by ψ is defined as the ratio of the normal and tangential stress at a distance $r=l$ such that

$$\psi=tan^{-1}\left[\frac{\sigma_{12}\left(r=l\right)}{\sigma_{22}\left(r=l\right)}\right]=tan^{-1}\left\{\frac{Im\left[\left(K_1+iK_2\right)l^{i\varepsilon}\right]}{Re\left[\left(K_1+iK_2\right)l^{i\varepsilon}\right]}\right\} \tag{17}$$

In order to obtain the phase angle associated with the characteristic length l, the interaction integral method is used to separate the mixed-mode stress intensity factors at the interfacial crack tip. In this study, the cohesive length is chosen as the characteristic length l. The factors K_1 and K_2 can be decomposed by using the interaction integral technique (Matos *et al*. 1989, Stem *et al*. 1976). It should be noted that the dimensions of the factors K_1 and K_2 are stress units time length units raised to the power 1/2-$i\varepsilon$. When the Dundurs parameter is zero, the real and imaginary parts of the stress intensity factor are uniquely identified as the mode I and mode II components of the stress intensity factor. The conversion of $K_I+iK_{II}=K\,l^{i\varepsilon}=\left|K\right|exp\left(i\psi\right)$ can be performed to obtain the stress intensity factors at the characteristic length l from the crack tip.

When the material interface is a plane, the energy release rate, J-integral (Rice 1968) which is path independent for the crack segment including the tip at the interface, can be expressed by

$$G=\frac{1}{H}\left(K_1^2+K_2^2\right) \tag{18}$$

where

$$\frac{1}{H}=\frac{1}{2cosh^2\left(\pi\varepsilon\right)}\left(\frac{1}{E_1^*}+\frac{1}{E_2^*}\right) \tag{19}$$

where $E_i^*=E_i$ for plane stress and $E_i^*=E_i/\left(1-\nu_i^2\right)$ for plane strain.

Most materials show that mode I fracture energy is different from mode II fracture energy. In describing an interface crack propagation, one may prescribe a relation between K_1 and K_2, which in general gives the critical energy release rate G_c as a function of the phase angle

$$G_c=G_c\left(\psi\right) \tag{20}$$

3.3 Mixed-mode cohesive laws

Cohesive zone models have been widely used in the numerical simulation of fracture processes

of materials for a variety of applications. Cohesive zone was originally proposed for the purpose of removing the crack-tip stress singularity (Barenblatt 1962). The fracture energy in a cohesive zone is the same as the critical energy release rate in linear elastic fracture mechanics when the stress singularity at the cohesive zone crack tip does not exist. Cohesive zone models can be applied to the interface crack between dissimilar materials by simply adding the shear traction and the corresponding shear separation in the cohesive law.

Xu and Needleman (1993) extended the exponential form of cohesive laws to predict a mixed-mode crack propagation combined normal and shear separations. Cohesive tractions are regarded as the function of uncoupled separations in normal and tangential directions. Fig. 4 illustrates a mixed-mode cohesive law expressed by normal and shear traction-separation relationships. Unlike this model, Tvergaard (1990) proposed a quadratic cohesive zone model with a coupling parameter in which the traction components are expressed as a function of the relative separations and this parameter. The parameter is introduced to characterize the interaction of normal and shear separations. Potential-based cohesive zone models (Needleman 1987, Freed and Banks-Sills 2008) have been proposed to impose different fracture energy with respect to the fracture mode. The derivatives of a potential with respect to the normal and shear separation result in the normal and shear cohesive tractions, respectively. Mixed-mode cohesive zone models provide a coherent analytical framework for fracture along interfaces that naturally incorporates both strength and energy criterion. The mode-I toughness (area under the normal traction-separation curve), and the mode-II toughness (area under the shear traction-separation) depend on the phase angle, which describe many of the important aspects of interfacial failure.

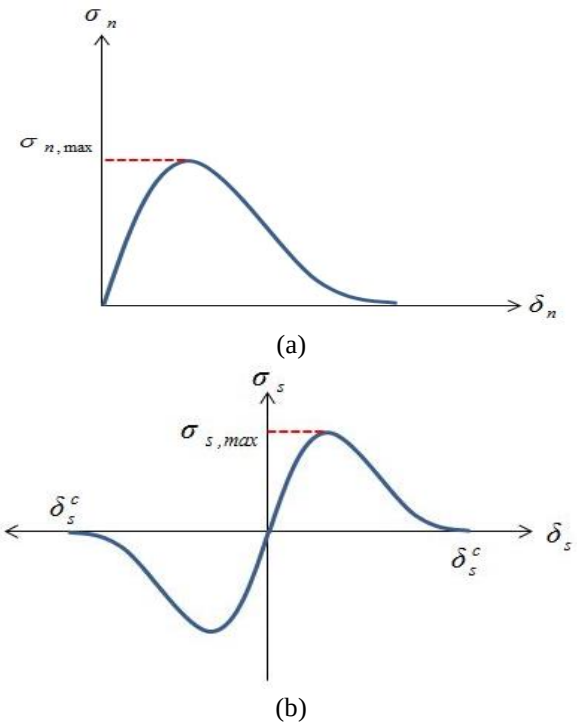

Fig. 4 Schematics of mixed-mode cohesive laws: (a) normal traction and separation, (b) shear traction and separation

4. Extraction of a mixed-mode cohesive law from measured displacements

In this section, the experimental and numerical processes are described to obtain a mixed-mode cohesive zone and the corresponding phase angle for a crack propagating along a bi-material interface. Cracked specimens were prepared by partially attaching epoxy and transparent thermoplastic (TR) resin mixtures. Displacements in a far-field region from the crack tip are measured by using digital image correlation (DIC) technique. Measured displacements are transferred from measurement locations to FE nodes by using moving least square (MLS) approximation. The same FE model is used to obtain numerical auxiliary fields of the interaction *J*- and *M*-integrals in the FPM. The inverse analyses are carried out to evaluate normal and shear cohesive tractions and separations in the cohesive zone at the interface. Mode mixity at the interfacial crack is also obtained by using the interaction integral technique.

4.1 Specimen preparation and displacement measurements

An interfacial crack between dissimilar materials is made by partially attaching two materials of epoxy and TR resin mixtures in a set of smooth cast. The geometry and dimensions of the double cantilever specimen with an interface crack between epoxy and TR resin mixtures is shown in Fig. 5. The thickness of the specimens is 2 mm. We choose that the mixture ratio of epoxy and hardener is 3:1 and the mixture ratio of TR resin-hardener is 10:8. The mechanical properties of epoxy and TR resin mixtures are obtained by taking tensile tests. Fig. 6 shows the stress-strain curves of the epoxy mixture and the TR resin mixture. The elastic modulus E and the Poisson's ratio v of the epoxy mixture are determined as E_1=5923.1 MPa and v_1=0.33, respectively. The elastic modulus E and the poisson's ratio v of the TR resin mixture are E_2=1836.3 MPa and v_2=0.3, respectively. In order to make a bi-material specimen, the epoxy mixture is poured into a mold made of silicon 1403. The epoxy mixture is cured at room temperature for 12 hours. Before TR resin mixture is poured into the other part, a laminating sheet made of aluminum is attached to debond some parts of interface between the two materials. The thickness of the laminating sheet is approximately 100 μm. TR resin mixture is then poured into the other mold to partially attach along the interface. In order to make a sharper interfacial crack, approximately 3000 cycles of a fatigue load are applied to the specimen.

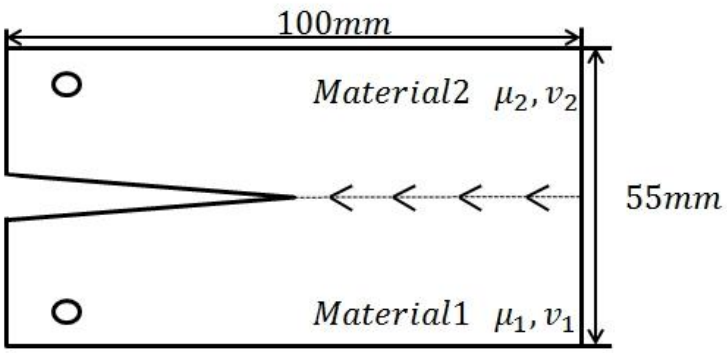

Fig. 5 Double cantilever specimen with an interface crack between dissimilar materials

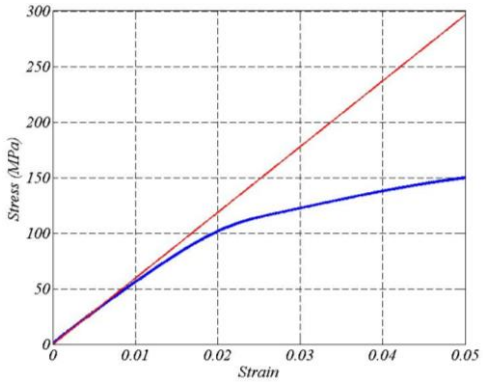

(a)

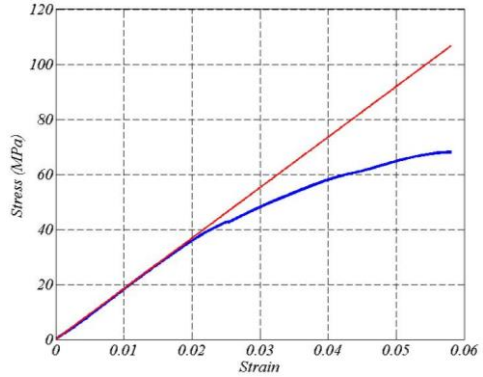

(b)

Fig. 6 Stress-strain curves of epoxy and TR resin mixtures: (a) epoxy mixture (the mixture ratio of epoxy and hardener=3:1), (b) TR resin mixture (the mixture ratio of resin and hardener is 10:8)

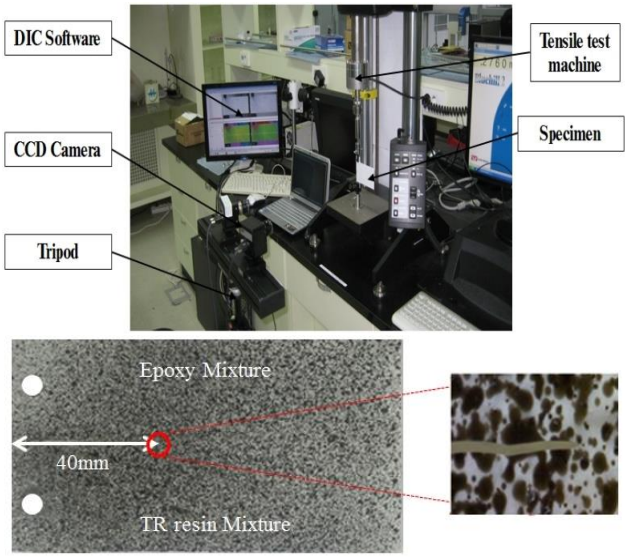

Fig. 7 Bi-material specimen with an initial crack and pin-holes for grips; the magnified image on the right is the initial crack shape observed by a microscope

The bi-material specimen with an initial crack is loaded by the micro-tensile test machine, as shown in Fig. 7. Displacement controlled loading is applied incrementally to the specimen. In order to measure displacement fields, we use a DIC system with two CCD cameras of full 0.8 mega pixels which are shown in Fig. 7.

4.2 A mixed-mode cohesive law extracted from measured displacements

The measured displacements at the centers of subsets in the DIC system are transferred to FE nodes by using MLS approximation. The subsets in the DIC system do not match with the nodes of a FE model for extracting crack-tip cohesive laws. Additionally, the measured displacements contain local fluctuations or measurement noises, which cause a deterioration of inverse solutions due to an inherent ill-conditioning of the inverse system even though a large subset size is set to reduce measurement noises. MLS approximation takes space-varying coefficients in the least square method with a basis and weight functions defined on influence domains. Accordingly, MLS approximation can reduce measurement noises to make the inverse process stable. Fig. 8 shows von-Mises stress distribution in the FE model of the bi-material specimen by imposing measured displacements. Linear elastic materials with the properties obtained by uniaxial tensile tests are applied to the FE analysis using the commercial code ABAQUS/standard. Since nonlinear deformations near the crack tip are large, the stresses in the local region near the crack tip are also large compared to the stresses in other regions, as shown in Fig. 8. It should be noted that the stresses near the crack tip are not actual values, because linear elastic materials are used in the FE simulation. In order to make the auxiliary fields $\hat{S}$, we give uniform traction to each element along the crack surfaces. A mixed-mode cohesive law can be then extracted by using the conservation of the interaction *J*- and *M*- integrals in Eqs. (5) and (6) with the numerical auxiliary fields. As indicated in Fig. 9, integral domains are taken by three different paths according to the distance from the crack-tip. Contour A includes non-linear deformations near the crack tip, which can result in different normal and shear cohesive laws from those obtained by using contours B and C. The size and the location of cohesive zone are determined to give positive normal tractions in the cohesive zone, which requires iterative computations of solving inverse equations.

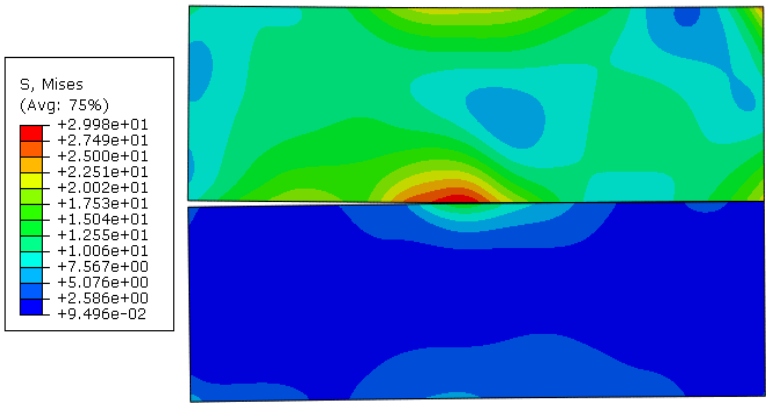

Fig. 8 von-Mises stress distribution in the finite element model of the bi-material specimen by imposing measured displacements; linear elastic properties of epoxy and TR resin mixtures are used in the finite element simulation

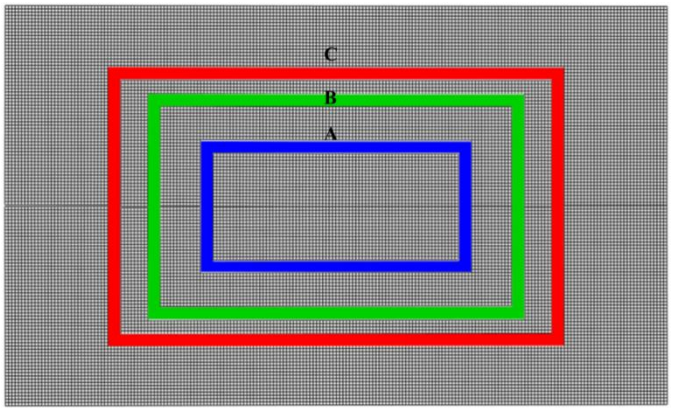

Fig. 9 Finite element mesh of the double cantilever specimen; the integration contours A, B and C are used for the calculation of the interaction *J*- and *M*- integrals

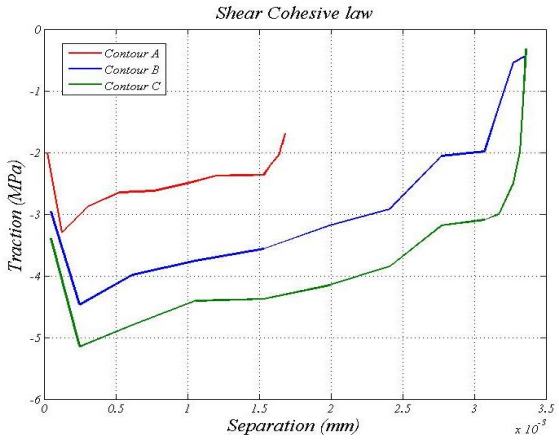

(b)

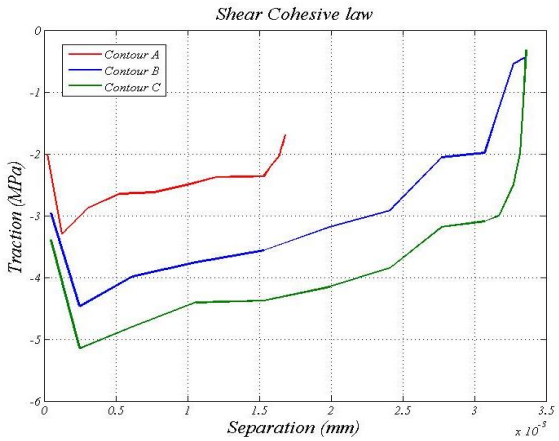

(c)

Fig. 10 Mixed-mode cohesive laws for an interface crack between epoxy and TR resin mixtures: normal cohesive traction and separation; (b) shear cohesive traction and separation

The solutions of Eqs. (10) and (11), which are inverse solutions to extract cohesive tractions and separations from measured displacements, are plotted in Fig. 10. The mixed-mode cohesive laws obtained by using contour A are different from those obtained by using contours B and C, because nonlinear deformations in contour A affect the right terms in Eqs. (10) and (11). The inverse solutions using contours B and C are not much different, which shows the path independency of the interaction *J*- and *M*-integrals evaluated from measured displacements. As a result, the mixed-mode cohesive laws for the interface crack between epoxy and TR resin mixtures can be determined from tractions and separations estimated by using contours B or C. Note that the cohesive energy and the maximum strength of the normal cohesive law are much higher than those in the shear cohesive law.

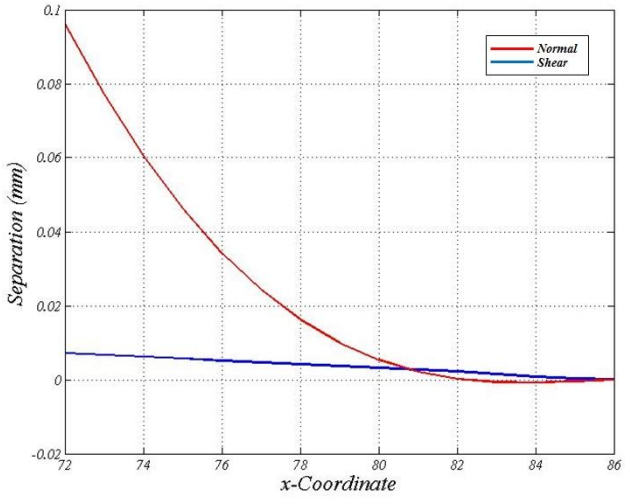

Fig. 11 Cohesive separations in the cohesive zone of the interface crack between epoxy and TR resin mixtures

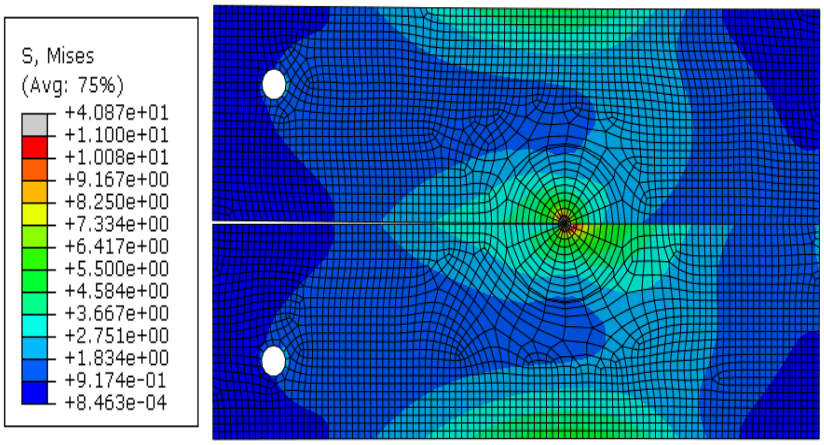

Fig. 12 von-Mises stress distribution in the finite element model of the bi-material specimen by applying loads in experiments

Cohesive normal and shear separations in the x-coordinate along the interface are plotted in Fig. 11. The normal and shear separations in the cohesive zone are similar regardless of contours for evaluating the interaction J- and M-integrals. As mentioned earlier, the size and the location of the cohesive zone are determined to give the positive normal cohesive tractions. The corresponding cohesive normal separations behind the cohesive crack tip are partially negative as shown in Fig. 11. Although the amount of penetration of the cohesive crack surfaces is very small, the possibility arises that mixed-mode cohesive laws with negative normal separations are required to remove singularities at the cohesive crack tip. A more sophisticated study is needed to elucidate mixed-mode cohesive laws for an interface crack between dissimilar materials.

In order to obtain the phase angle of the interface crack, a FE model of the cantilever beam specimen is solved by applying the loads in experiments. Linear elastic properties are used in the FE analysis, and von-Mises stress distribution in the FE model is plotted in Fig. 12. Stress intensity factors K_1 and K_2 in Eq. (12) are obtained by using the interaction integral technique (Matos *et al*. 1989, Stem *et al*. 1976) in ABAQUS/Standard. The stress intensity factors of the interface crack are K_1=21.91 MPa mm$^{1/2}$ and K_2=-4.713 MPa mm$^{1/2}$. The characteristic length in Eq. (17) is chosen as the cohesive length in this study. Finally, the phase angle of the interface crack between epoxy and TR resin mixtures is calculated as ψ=-15.126°.

5. Conclusions

The extraction of crack-tip cohesive laws from measured displacements in a far field through an inverse analysis is a challenging problem, especially for a mixed-mode condition of interface crack between dissimilar materials. In this study, we use a hybrid method which is an efficient computational inverse analysis, using experimentally measured displacements and the numerical auxiliary fields by imposing uniform tractions along the crack face in a finite element model. The path-independent interaction J- and M-integrals between these auxiliary fields and the measurement displacements are used to extract the mixed-mode cohesive laws of an interface crack between epoxy and TR resin mixtures. It is emphasized that the contour path should not include nonlinear deformations near the crack tip in order to obtain proper cohesive tractions and separations in the cohesive zone. A penetration of cohesive crack surfaces behind the cohesive crack tip is obtained in this study, which remains a possibility of mixed-mode cohesive laws with negative normal separations for an interface crack to remove singularities at the cohesive crack tip. In addition, the phase angle of the mixed-mode cohesive law is evaluated to characterize the interface crack between epoxy and TR resin mixtures. The proposed procedure can be an efficient and effective method to estimate mixed-mode cohesive laws of interface cracks by combining experimental tests and numerical simulations.

Acknowledgements

This work was supported by the Technology Innovation Program (10048305, Launching Plug-in Digital Analysis Framework for Modular system Design) funded by the Ministry of Trade, Industry & Energy (MI, Korea).

References

Williams, M.L. (1959), "The stresses around a fault or crack in dissimilar media", *Bull. Seismol. Soc. Am.*, **49**(2), 199-204.

Rice, J.R. (1988), "Elastic fracture mechanics concepts for interfacial cracks", *J. Appl. Mech*., ASME, **55**(1), 98-103.

Erdogan, F. (1965), "Stress distribution in bonded dissimilar materials with cracks", *J. Appl. Mech*., ASME **32**(2), 403-10.

England, A.H. (1965), "A crack between dissimilar media", *J. Appl. Mech*., ASME, **32**(2), 400-402.

Rice, J.R. and Sih, G.C. (1965), "Plane problems of cracks in dissimilar media", *J. Appl. Mech*., ASME, **32**(2), 418-423.

Matos, P.P.L., Mcmeeking, R.M., Charalambides, P.G. and Drory, M.D. (1989), "A method for calculating stress intensities in bimaterial fracture", *Int. J. Fract.*, **40**(4), 235-254.

Hutchinson, J.W. and Suo, Z. (1992), "Mixed mode cracking in layered materials", *J. Appl. Mech*., **29**(63), 191.

Xu, X.P. and Needleman, A. (1994), "Numerical simulations of fast crack growth in brittle solids", *J. Mech. Phys. Solids*., **42**(9), 1397-1434.

Camacho, G.T. and Ortiz, M. (1996), "Computational modeling of impact damage in brittle materials", *Int. J. Solid. Struct*., **33**(20), 2899-2938.

Ortiz, M. and Pandolfi, A. (1999), "Finite-deformation irreversible cohesive elements for three-dimensional crack-propagation analysis", *Int. J. Numer. Method. Eng*., **44**, 1267-1282.

Mergheim, J., Kuhl, E. and Steinmann, P. (2005), "A finite element method for the computational modeling of cohesive cracks", *Int. J. Numer. Meth. Eng*., **63**(2), 276-289.

Xu, L. and Tippur, H.V. (1995), "Fracture parameters for interface cracks: an experimental-finite element study of crack tip fields and crack initiation toughness", *Int. J. Fract*., **71**(4), 345-363.

Ikeda, T., Miyazaki, N. and Soda, T. (1998), "Mixed mode fracture criterion of interface crack between dissimilar materials", *Eng. Fract. Mech*., **59**(6), 725-735.

Liechti, K.M. and Chai, Y.S. (1992), "Asymmetric shielding in interfacial fracture under in-plane shear", *J. Appl. Mech*., ASME, **59**(2), 295-304.

Yuuki, R., Liu, J., Xu, Q., Ohira, J.Q. and Ono, T. (1994), "Mixed mode fracture criteria for an interface crack", *Eng. Fract. Mech.*, **47**(3), 367-377.

Tan, H., Liu, C., Huang, Y. and Geubelle, P.H. (2005), "The cohesive law for the particle/matrix interfaces in high explosives", *J. Mech. Phys. Solid*., **53**(8), 1892-1917.

Zhu, Y., Liechti, K.M. and Ravi-Chandar, K. (2009), "Direct extraction of rate-dependent traction-separation laws for polyurea/steel interfaces", *Int. J. Solid. Struct*., **46**(1), 31-51.

Guo, Z.K., Kobayashi, A.S., Hay, J.C. and White, K.W. (1999), "Fracture process zone modeling of monolithic Al2O3", *Eng. Fract. Mech*., **63**(2), 115-129.

Shen, B. and Paulino, G.H. (2011), "Direct extraction of cohesive fracture properties from digital image correlation: A hybrid inverse technique", *Exp. Mech*., **51**(2), 143-163.

Gain, A.L., Carroll, J., Paulino, G.H. and Lambros, J. (2011), "A hybrid experimental/numerical technique to extract cohesive fracture properties for mode-I fracture of quasi-brittle materials", *Int. J. Fract*., **169**(2), 113-131.

Kim, H.G. and Lee, K.W. (2009), "A study on the influence of measurement location and regularization on the evaluation of boundary tractions by inverse finite element method", *Finite Elem. Anal. Des.*, **45**(8), 569-582.

Hong, S. and Kim, K.S. (2003), "Extraction of cohesive-zone laws from elastic far-fields of a cohesive crack tip: a field projection method", *J. Mech. Phys. Solid*., **51**(7), 1267-1286.

Hong, S., Chew, H.B. and Kim, K.S. (2009), "Cohesive-zone laws for void growth - I. Experimental field projection of crack-tip crazing in glassy polymers", *J. Mech. Phys. Solid*., **57**(8), 1357-1373.

Chew, H.B., Hong, S. and Kim, K.S. (2009), "Cohesive zone laws for void growth - II. Numerical field

projection of elasto-plastic fracture processes with vapor pressure", *J. Mech. Phys. Solid.*, **57**(8), 1374-1390.
Chalivendra, V.B., Hong, S., Arias, I., Knap, J., Rosakis, A. and Ortiz, M. (2009), "Experimental validation of large-scale simulations of dynamic fracture along weak planes", *Int. J. Impact Eng*., **36**(7), 888-898.
Kim, H.G., Chew, H.B. and Kim, K.S. (2012), "Inverse extraction of cohesive zone laws by field projection method using numerical auxiliary fields", *Int. J. Numer. Meth. Eng.*, **91**(5), 516-530.
Oh, J.C. and Kim, H.G. (2013), "Inverse estimation of cohesive zone laws from experimentally measured displacements for the quasi-static mode I fracture of PMMA", *Eng. Fract. Mech*., **99**, 118-131.
Shih, C.F., Moran, B. and Nakamura, T. (1986), "Energy release rate along a three-dimensional crack front in a thermally stresses body", *Int. J. Fract*., **30**(2), 79-102.
Jin, Z-.H. and Sun, C.T. (2005), "Cohesive zone modeling of interface fracture in elastic bi-materials", *Eng. Fract. Mech*., **72**(12), 1805-1817.
Rice, J.R. (1988), "Elastic fracture mechanics concepts for interface cracks", *J. Appl. Mech*., ASME, **55**(1), 98-103.
Matos, P.P.L., McMeeking, R.M., Charalambides, P.G. and Drory, M.D. (1989), "A method for calculating stress intensities in biomaterial fracture", *Int. J. Fract*., **40**(4), 235-254.
Stern, M., Becker, E.B. and Dunham, R.S. (1976), "A contour integral computation of mixed-mode stress intensity factors", *Int. J. Fract.*, **12**(3), 359-368.
Rice, J.R. (1968), "A path independent integral and the approximate analysis of strain concentration by notches and cracks", *J. Appl. Mech*., ASME, **35**(2), 379-386.
Barenblatt, G.I. (1962), "The mathematical theory of equilibrium cracks in brittle fracture", *Adv. Appl. Mech*., **7**(1), 55-129.
Xu, X.P. and Needleman, A. (1993), "Void nucleation by inclusion debonding in a crystal matrix", *Model. Simul. Mater. Sci. Eng*., **1**(2), 111-132.
Tvergaard, V. (1990), "Effect of fibre debonding in a whisker-reinforced metal", *Mater. Sci. Eng*., **125**(2), 203-213.
Needleman, A. (1987), "A continuum model for void nucleation by inclusion debonding", *J. Appl. Mech*., ASME, **54**(3), 525-531.
Freed, Y. and Banks-Sills, L. (2008), "A new cohesive zone model for mixed mode interface fracture in biomaterials", *Eng. Fract. Mech*., **75**(15), 4583-4593.
Park, K.S., Paulino, G.H. and Roesler, J.R. (2009), "A unified potential-based cohesive model of mixed-mode fracture", *J. Mech. Phys. Solid*., **57**(6), 891-908.

MC